Satiety factor oleoylethanolamide recruits the brain histaminergic system to inhibit food intake

Gustavo Provensi[a,1], Roberto Coccurello[b,1], Hayato Umehara[a,2], Leonardo Munari[a,3], Giacomo Giacovazzo[b], Nicoletta Galeotti[a], Daniele Nosi[c], Silvana Gaetani[d], Adele Romano[d], Anna Moles[b], Patrizio Blandina[a], and Maria Beatrice Passani[a,4]

[a]Dipartimento di Neuroscienze, Psicologia, Area del Farmaco, e Salute del Bambino, Sezione di Farmacologia e Tossicologia, Università di Firenze, 50139 Florence, Italy; [b]Institute of Cell Biology and Neurobiology, National Research Council/Fondazione Santa Lucia, 00143 Rome, Italy; [c]Dipartimento di Medicina Sperimentale e Clinica, Università di Firenze, 50134 Florence, Italy; and [d]Dipartimento di Fisiologia e Farmacologia V. Erspamer, Sapienza Università di Roma, 00185 Rome, Italy

Edited* by Ivan Izquierdo, Pontifical Catholic University of Rio Grande do Sul, Porto Alegre, Brazil, and approved June 27, 2014 (received for review November 26, 2013)

Key factors driving eating behavior are hunger and satiety, which are controlled by a complex interplay of central neurotransmitter systems and peripheral stimuli. The lipid-derived messenger oleoylethanolamide (OEA) is released by enterocytes in response to fat intake and indirectly signals satiety to hypothalamic nuclei. Brain histamine is released during the appetitive phase to provide a high level of arousal in anticipation of feeding, and mediates satiety. However, despite the possible functional overlap of satiety signals, it is not known whether histamine participates in OEA-induced hypophagia. Using different experimental settings and diets, we report that the anorexiant effect of OEA is significantly attenuated in mice deficient in the histamine-synthesizing enzyme histidine decarboxylase (HDC-KO) or acutely depleted of histamine via interocerebroventricular infusion of the HDC blocker α-fluoromethylhistidine (α-FMH). α-FMH abolished OEA-induced early occurrence of satiety onset while increasing histamine release in the CNS with an H_3 receptor antagonist-increased hypophagia. OEA augmented histamine release in the cortex of fasted mice within a time window compatible to its anorexic effects. OEA also increased c-Fos expression in the oxytocin neurons of the paraventricular nuclei of WT but not HDC-KO mice. The density of c-Fos immunoreactive neurons in other brain regions that receive histaminergic innervation and participate in the expression of feeding behavior was comparable in OEA-treated WT and HDC-KO mice. Our results demonstrate that OEA requires the integrity of the brain histamine system to fully exert its hypophagic effect and that the oxytocin neuron-rich nuclei are the likely hypothalamic area where brain histamine influences the central effects of OEA.

histamine receptors | behavioral satiety sequence | BSS | paraventricular hypothalamic nuclei | PVN

Eating behavior is regulated by central neurotransmitter systems and peripheral stimuli that interact to change the behavioral state and concur to alter homeostatic aspects of appetite and energy expenditure. The fatty acid amide oleoylethanolamide (OEA) is released by the small intestine in a stimulus-dependent manner and suppresses food intake by activating peroxisome proliferator-activated receptor-α (PPAR-α) (1). Systemic administration of OEA induces c-Fos mRNA expression through the vagus nerve to the nucleus of the solitary tract (NST), supraoptic nuclei (SON), and paraventricular hypothalamic nuclei (PVN) and increases the expression of oxytocin (2, 3), which is involved in the central coordination of homeostatic signals and feeding behavior (4). However, it is not known whether OEA recruits other neurotransmitter systems in the brain to reduce food intake. Histaminergic neurons are clustered in the hypothalamic tuberomammillary nuclei (TMN). They send projections organized in functionally distinct circuits impinging on different brain regions (5), and their firing frequency changes according to the behavioral state (6). Brain histamine plays a fundamental role in eating behavior as it induces loss of appetite and has long been considered a satiety signal that is released during food intake (7). Early studies showed that treatments increasing brain histamine availability or activating histamine H_1 receptor (H_1R) in the CNS suppressed food intake (8–10), and enhanced c-Fos–like immunoreactivity in the PVN (10), whereas H_1R blockade in the ventromedial hypothalamus (VMH) increased both meal size and duration, and suppressed the activity of glucose-responding neurons (11).

With these considerations in mind, we examined the hypothesis that peripherally administered OEA engages histamine signaling in the brain. We assessed the effect of OEA on cumulative food intake as well as on the expression of the behavioral satiety sequence (BSS) in mice defective in brain histamine, either because they lack the histamine-synthesizing enzyme histidine decarboxylase (HDC) or because acutely deprived of histamine by interocerebroventricular (i.c.v.) infusion of HDC inhibitor α-fluoromethylhistidine (α-FMH). We also assessed the effect of OEA following systemic administration of the H_3R antagonist ABT-239 that transiently increases

Significance

Several endogenous molecules contribute to the building of a complex network of neural and hormonal signals that align food intake and energy expenditure. Cerebral histamine works as a satiety factor by activating histamine H_1 receptor (H_1R) in specific hypothalamic nuclei. Indeed, atypical antipsychotics presumably cause obesity by targeting brain H_1R. The endogenous lipid messenger oleoylethanolamide (OEA) mediates fat-induced satiety by engaging sensory fibers of the vagus nerve that project centrally. We find that depletion of brain histamine blunts OEA-induced hypophagia in mice. Our study uncovers previously unidentified neural signaling mechanisms involved in the anorectic action of OEA. Our data offer new perspectives for developing more effective and safer pharmacotherapies to treat obesity and ameliorate the profile of centrally acting drugs.

Author contributions: G.P., R.C., H.U., L.M., N.G., A.M., P.B., and M.B.P. designed research; G.P., R.C., H.U., L.M., G.G., D.N., A.R., and M.B.P. performed research; S.G., A.R., and P.B. contributed new reagents/analytic tools; G.P., R.C., H.U., L.M., G.G., N.G., D.N., S.G., A.M., and M.B.P. analyzed data; and G.P., R.C., and M.B.P. wrote the paper.

The authors declare no conflict of interest.

*This Direct Submission article had a prearranged editor.

[1]G.P. and R.C. contributed equally to this work.

[2]Present address: Division of Pharmacology, Graduate school of Medical and Dental Science, Niigata University, Niigata 951-8510, Japan.

[3]Present address: Department of Pharmacology and Systems Therapeutics, Mount Sinai School of Medicine, New York, NY 10029.

[4]To whom correspondence should be addressed. Email: beatrice.passani@unifi.it.

The work was presented in part at the 41st Annual Meeting of the Histamine Society, Belfast, United Kingdom, May 2–6, 2012.

This article contains supporting information online at www.pnas.org/lookup/suppl/doi:10.1073/pnas.1322016111/-/DCSupplemental.

brain histamine release (12). Finally, we determined changes in neuronal activity by assessing the pattern of c-Fos expression induced by OEA in hypothalamic brain regions controlling feeding behavior and in brain regions regulating the motivational aspect of foraging in both HDC-KO and WT littermates. Our findings revealed that the anorexic effects of OEA are blunted in brain histamine-deficient mice, and establish new functional connections between peripherally acting hypophagic signals and brain histamine neurotransmission.

Results

Interaction Between Brain Histamine and OEA on Food Consumption. To test whether the integrity of the histaminergic system contributes to the anorexiant effect of OEA, we used HDC-KO mice, which are unable to synthesize histamine. OEA was injected i.p. at 10 mg/kg to induce long-lasting appetite suppression (1); it does not readily enter the CNS (13) and does not cause taste aversion (14). Controls received equivalent volumes of the vehicle. OEA caused a profound reduction of the total amount of food consumed by WT mice compared with vehicle-treated littermates within the first 60 min after injection ($P < 0.001$; Fig. 1*A*). Two-way ANOVA revealed an overall significant difference between groups [$F_{(\text{time})4,170} = 133.14$, $P < 0.0001$; $F_{(\text{treatment})3,170} = 185.64$, $P < 0.0001$; $F_{(\text{time} \times \text{treatment})12,170} = 12.93$, $P > 0.0001$]. As expected, vehicle-treated HDC-KO mice consumed comparable amounts of food with respect to WT animals (histamine-deficient mice are not hyperphagic, nor obese up to 12 wk of age) (15), whereas the anorexic effect of OEA was significantly diminished in HDC-KO mice ($P < 0.01$ at 45 min; $P < 0.001$ at 60 min). The effect of OEA was short lived as no difference in food consumption was observed among experimental groups 4 h after OEA injection. Histamine-deficient mice develop metabolic changes with age (15). Hence, to exclude the involvement of compensatory mechanisms in HDC-KO mice, we measured food intake also in CD1 mice that received an i.c.v. infusion of the HDC suicide inhibitor α-FMH at a dose that abolishes basal and stimulated histamine release (see Fig. 3*B*). Mice were tested at lights off (1900 h), when they have a greater incentive to eat and the activity of histamine neurons is higher (16). Two-way ANOVA revealed an overall significant difference among groups [$F_{(\text{treatment})3,104} = 20.67$, $P < 0.0001$; $F_{(\text{time})4,104} = 121.36$, $P < 0.00001$; $F_{(\text{time} \times \text{treatment})12,104} = 13.30$, $P < 0.0001$]. OEA caused a profound reduction in the total amount of food consumed by CD1 mice that received an i.c.v. infusion of saline (Fig. 1*B*). Mice in the α-FMH/vehicle group tended to eat more than the saline/vehicle animals, although this effect did not reach statistical significance. In α-FMH–treated mice, OEA-induced hypophagia was significantly less prominent than in the saline/OEA group. The effect reached statistical significance 45 min after OEA injection ($P < 0.01$). The overall trend is very similar to the results obtained with HDC-KO mice during the lights-on phase, although during the lights-off phase all experimental groups ate consistently larger amounts of food. We then argued that, if OEA modulates feeding by recruiting the central histamine system, augmenting histamine release pharmacologically would potentiate the anorexic effect of exogenous OEA. We measured food-consumption in 12 h-fasted CD1 mice treated with a combination of OEA (10 mg/kg) and ABT-239 (3 mg/kg), an H_3R antagonist that increases histamine release by blocking H_3 autoreceptors (12). Two-way ANOVA followed by Bonferroni's post hoc test revealed a significant difference between groups [$F_{(\text{time})4,104} = 392.5$, $P < 0.0001$; $F_{(\text{treatment})3,104} = 31.81$, $P < 0.0001$; $F_{(\text{time} \times \text{treatment})12,104} = 29.04$, $P < 0.0001$]. Each compound significantly decreased food intake and coadministration of compounds determined a further decrease ($P < 0.01$ at 45 min and $P < 0.001$ at 60 min; Fig. 1*C*). We then determined the type of interaction between the two compounds by performing an isobolographic analysis as described in *SI Materials and Methods*. We observed a dose-dependent hypophagic effect for each compound and for OEA–ABT-239 mixtures administered in fixed ratios (Fig. S1). The ED_{50} and 95% confidence interval, obtained from regressions of dose–response curves (Fig. 1 *D* and *E*), were (in milligrams per kilogram) $ED_{50\text{ABT-239}} = 3.262$ (2.883–3.641), $ED_{50\text{OEA}} = 5.283$ (4.836–5.731), and $ED_{50\text{mix}} = 4.389$ (3.727–5.050). In the isobologram, the dose of ABT-239 needed to reach 50% of the effect is plotted on the abscissa and the isoeffective dose of OEA on the ordinate (Fig. 1*F*). The straight line connecting these two points represents the theoretical additive effect. A Student *t* test revealed no significant differences between the experimental $ED_{50\text{mix}}$ and the theoretical $ED_{50\text{add}} = 4.275$ (3.731–4.813). Furthermore, the interaction index $\gamma = 1.03$ indicates an additive interaction between OEA and ABT-239 (17).

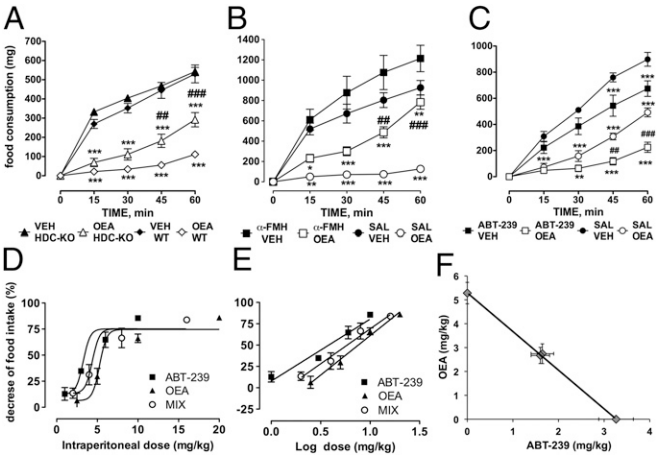

Fig. 1. Interactions between OEA and brain histamine on food consumption. (*A*). Time course of the effect of systemic administration of OEA (10 mg/kg, i.p.) or vehicle (VEH) on cumulative food intake in 12 h-fasted HDC-KO and WT mice during the lights-on period (0900 h). Each point represents mean ± SEM of 11–8 mice. $^{***}P < 0.001$ vs. respective controls. $^{###}P < 0.001$; $^{##}P < 0.01$ vs. OEA-treated mice WT or HDC-KO mice by two-way ANOVA and Bonferroni's test. (*B*) Time course of the effect of α-FMH administration (5 μg; i.c.v.) or saline (SAL) on OEA-suppressed food intake in 12 h-fasted mice. Each point represents mean cumulative food consumption ± SEM of seven to eight mice during the lights-off period (1900 h). $^{***}P < 0.001$, $^{**}P < 0.01$, $^{*}P < 0.5$ vs. respective controls; $^{##}P < 0.01$, $^{#}P < 0.05$ vs. OEA-treated WT or α-FMH–injected mice; two-way ANOVA and Bonferroni's test. (*C*) Increased brain histamine boosts OEA-induced suppression of food intake. Time course of 10 mg/kg OEA and 3 mg/kg ABT-239 effects on cumulative food intake in 12 h-fasted CD1 mice during the lights-on period (0900 h). Each point represents mean ± SEM of seven to eight mice. $^{***}P < 0.001$, $^{**}P < 0.01$, OEA and ABT-239 vs. respective controls; $^{###}P < 0.001$; $^{##}P < 0.01$, ABT-239/OEA vs. saline/OEA. (*D* and *E*) Sigmoidal and log-derived dose–response curves for OEA, ABT-239, and the combined compounds. Each point represents mean cumulative food consumption ±SEM of seven to nine mice expressed as percent food consumption of vehicles. (*F*) Isobologram for OEA–ABT-239 combined effects on food consumption.

Palatable Wet Mesh Intake and Time Spent Eating in Histamine-Depleted Mice. Palatable wet mesh (PWM) consumption was measured in α-FMH i.c.v.-infused mice treated with OEA during lights off. This protocol allowed us to use the BSS paradigm to disclose the specificity of potential anorexiant agents on satiety development (18). One-way ANOVA revealed a significant treatment effect on PWM intake ($F_{5,39} = 16.95$, $P < 0.0001$; Fig. 2*A*) during the 40-min BSS testing. α-FMH had no effect on consumed PWM. Post hoc comparisons revealed a significant decrease of PWM intake in saline/OEA (5 mg/kg, $P < 0.01$; 10 mg/kg, $P < 0.001$) groups compared with controls. α-FMH–infused mice treated with OEA did not significantly differ from

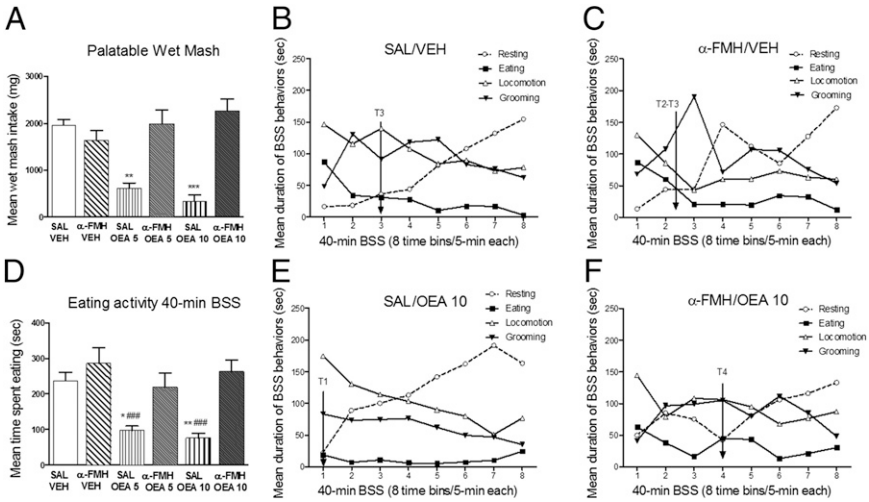

Fig. 2. Effects of OEA on the BSS in normal and histamine-depleted mice. *A* and *D* show mean cumulative PWM intake (±SEM) and mean time spent in eating activity (±SEM) over the 40-min BSS, respectively (n = 8 for each experimental group). *A* and *D* also illustrate the temporal development of eating, locomotion, grooming, and resting duration (seconds) in saline/vehicle (*B*), α-FMH/vehicle (*C*), saline/10 mg/kg OEA (*E*), and α-FMH/10 mg/kg OEA (*F*). Represented on the x axes are eight time bins (T) of 5 min each for a total of 40 min of BSS analysis. $^{***}P < 0.001$, $^{**}P < 0.01$, $^{*}P < 0.05$ vs. respective controls; $^{\#\#\#}P < 0.001$ vs. α-FMH/vehicle treated mice by one-way ANOVA and Bonferroni's test. Experiments were carried out during the lights-off period (1900 h).

controls in the amount of PWM consumed (Fig. 2*A*). Moreover, one-way ANOVA disclosed a significant treatment effect on time spent eating over the 40-min BSS test ($F_{5,39} = 8.60$, $P < 0.0001$; Fig. 2*D*). Post hoc analysis showed a significant decrease in total time spent eating only in saline/OEA (5 and 10 mg/kg) groups, compared with saline/vehicle and α-FMH/vehicle groups (Fig. 2*D*). No significant effects of OEA were detected in histamine-depleted mice compared with controls.

Effect of OEA on BSS Development in Histamine-Depleted Mice. We tested the effect of histamine depletion on the BSS in mice infused i.c.v. with α-FMH. Two-way ANOVA showed the significant main effect of time for all of the behavioral categories examined (eating, $F_{7,273} = 8.06$, $P < 0.0001$; locomotion, $F_{7,273} = 13.72$, $P < 0.0001$; resting, $F_{7,273} = 18.15$, $P < 0.0001$; and grooming $F_{7,273} = 4.13$, $P < 0.001$). The time-dependent changes in the evolution of these behavioral patterns reflect the gradual decline of active behaviors (i.e., eating, grooming, and locomotion) and the parallel increase in resting that typically describe the expression of the BSS (Fig. 2 *B*, *C*, *E*, and *F* and Fig. S2 *A* and *B*). One-way ANOVA for each behavior revealed a significant treatment effect only for the duration of eating during 40-min BSS testing (Fig. 2). Post hoc comparisons performed on the duration of eating showed that only saline/OEA groups (Fig. 2*E* and Fig. S2*A*) significantly reduced such activity compared with saline/vehicle and α-FMH/vehicle groups (Fig. 2 *B* and *C*). No significant effects of treatment on time spent resting [$F_{5,39} = 0.79$, not significant (n.s.)], motor ($F_{5,39} = 0.59$, n.s.), or grooming activities ($F_{5,39} = 1.81$, n.s.) were found among all experimental groups. As shown in BSS temporal patterns, both control groups displayed an initial peak of feeding response followed by its decline over time and subsequent transition to resting that gradually increased around time bin T3 (Fig. 2 *B* and *C*). This temporal pattern was different in mice with intact brain histamine treated with OEA (Fig. 2*E* and Fig. S2*A*). OEA administration produced a shifting of about 10-min of satiety and resting cooccurrence, thus emphasizing the premature onset of satiety in these animals with resting rapidly replacing eating activity (from a T3 to T1 interval) in a basically well-preserved BSS structure. In contrast, infusion of α-FMH prevented the effects of OEA on satiety onset, as shown in Fig. 2*F* and Fig. S2*B*.

Functional Interaction Between OEA and Brain Histamine. In line with the idea that OEA may exert its anorectic effects by modulating brain histamine signaling, we found that systemic administration of 10 mg/kg OEA increased histamine release from the prefrontal cortex by ∼160%. Furthermore, OEA increased histamine release only in 12 h-fasted but not in satiated mice (Fig. 3*A*). The increase in histamine was transient and reached a maximum within 30 min of OEA administration. Mean spontaneous histamine release was not significantly different between experimental groups (53.7 ± 18.8 fmol per 30 min-fasted mice; 61.9 ± 33 fmol per 30 min-fed ad libitum mice). We then measured histamine release from the prefrontal cortex of freely moving mice that received i.p. administration of 3 mg/kg ABT-239. As shown in Fig. 3*B*, ABT-239 increased significantly histamine release by ∼130%. Histamine mean spontaneous release was 49 ± 12 fmol/30 min. Coadministration of OEA and ABT-239 further increased cortical histamine release (Fig. 3*B*). Two-way ANOVA followed by Bonferroni's post hoc test showed a significant main effect between groups [$F_{(\text{treatment})1,61} = 6.12$, $P < 0.01$; $F_{(\text{time})8,61} = 11.6$, $P < 0.0001$; and $F_{(\text{treatment} \times \text{time})8,61} = 1.37$, n.s.]. Mean spontaneous histamine release was 34.3 ± 14.1 fmol/30 min. To ascertain whether our α-FMH protocol caused a prolonged depletion of releasable histamine stores from the mouse brain, we measured histamine release from the mouse cortex 24 h after α-FMH i.c.v. infusion. Cortical basal histamine contents of α-FMH–treated mice were below detection level and no further histamine release was elicited when mice received ABT-239 (Fig. 3*B*).

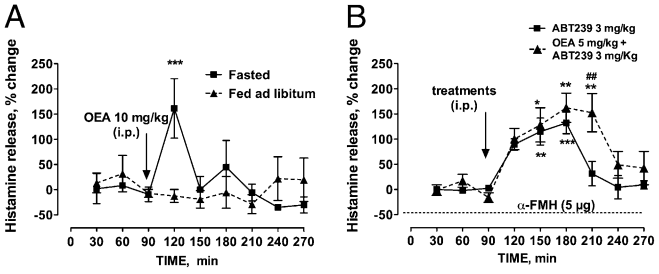

Fig. 3. Functional interaction between brain histamine and OEA. (*A*) Effect of OEA administration on histamine release in the prefrontal cortex of freely moving mice. Represented are means ± SEM of three fasted and four fed ad libitum mice. (*B*) Effect of ABT-239 and OEA–ABT-239 on cortical histamine release in freely moving mice. Represented are means ± SEM of four and five mice, respectively. ABT-239 and OEA were administered i.p. separately and α-FMH (5 μg) was administered i.c.v. Baseline histamine release was not detectable in α-FMH–treated mice or during ABT-239 administration (dashed line; n = 4). Experiments were carried out between 0900 and 1600 h. $^{***}P < 0.001$, $^{**}P < 0.01$, $^{*}P < 0.05$, vs. baseline values; $^{\#\#}P < 0.01$ vs. ABT-239, two-way ANOVA and Bonferroni's test. For clarity, we reported only the significant differences vs. the last baseline sample before drug treatment, although differences were significant vs. all baseline samples.

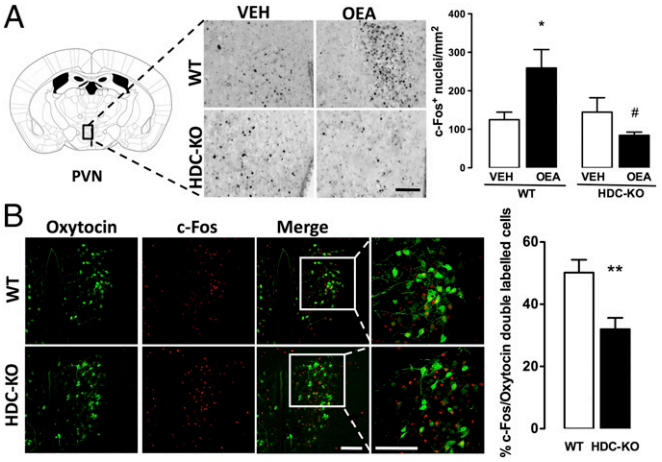

Fig. 4. OEA-induced c-Fos expression in the hypothalamic PVN nucleus is blunted in HDC-KO mice. (*A*) Brain coronal sections showing the effect of vehicle or 10 mg/kg OEA on c-Fos protein expression in WT and HDC-KO mice in PVN. (Scale bar: 100 μm.) Quantitative data are expressed in the bar graphs as means ±SEM; $*P < 0.05$ vs. respective controls; $^{\#}P < 0.05$ vs. WT/OEA by one-way ANOVA and Newman–Keuls test. (*B*) Immunohistochemical detection of oxytocin and c-Fos in the PVN neurons of WT and HDC-KO mice treated with OEA. (Scale bar: 50 μm.) The bar graph shows the percentage of oxytocin-immunopositive neurons expressing c-Fos in OEA-treated WT and HDC-KO mice; $**P < 0.01$, unpaired *t* test. $n = 3$–5 mice per experimental group.

OEA-Induced c-Fos Expression in HDC-KO Mice. In an attempt to clarify how brain histamine deficit may prevent the satiety effect of OEA, we measured c-Fos protein expression in the brain of HDC-KO and WT mice following OEA administration. OEA did not change c-Fos expression in the VMH ($F_{3,18} = 0.081$, n.s.) of either WT or HDC-KO mice (Fig. S3*C*). As expected from previous results obtained in rats (2), systemic OEA increased significantly c-Fos expression in the PVN of WT mice (Fig. 4*A*; $F_{3,18} = 4.817$, $P < 0.05$), whereas no differences were found in the PVN of HDC-KO mice treated with vehicle or OEA. OEA activates preferentially oxytocin neurons in the PVN (2). We found that the percentage of oxytocin neurons expressing c-Fos immunofluorescence was significantly lower in the PVN of OEA-treated HDC-KO mice compared with OEA-treated WT mice (Fig. 4*B*; $P < 0.01$), despite HDC-KO mice expressing higher levels of oxytocin-positive neurons (WT = 166 ± 17 per square millimeter vs. HDC-KO = 235 ± 14 per square millimeter; $P < 0.01$, unpaired *t* test). We also evaluated c-Fos expression in limbic brain structures related to feeding behavior that receive histaminergic innervation. Interestingly, in the nucleus accumbens that receives TMN input regulating exploratory behavior (19) indispensable during food provisioning, OEA administration decreased c-Fos expression in both HDC-KO and WT mice ($F_{3,16} = 5{,}550$, $P < 0.05$; Fig. S3*B*). In the infralimbic cortex, which presumably implements arousal during appetitive behavior (20) and provides the TMN with an essential input for the appetitive function of histaminergic neurons (21), no differences were found in c-Fos expression in either WT or HDC-KO mice receiving OEA (Fig. S3*A*). We also observed a significant increase in the percentage of c-Fos positive TMN neurons in OEA- compared with vehicle-treated WT mice (OEA = 12.1 ± 1.35%; vehicle = 5.4 ± 1.4%; $P < 0.01$, unpaired *t* test; Fig. S4).

Discussion

Satiety-related signals are integrated at the cellular and system level to give reliable and appropriate behavioral responses by recruiting specific neuronal populations. OEA is synthesized in several peripheral tissues and in the CNS (22) and in mammals it has been described as a mediator of numerous metabolic processes (4). OEA secreted by enterocytes serves as a fat-sensing molecule that signals to satiety centers in the brain by engaging vagus nerve sensory fibers (2, 4, 23) and suppresses feeding by indirectly activating central oxytocin transmission in the PVN and SON (3). However, it is not known if other neurotransmitter systems integrate the peripheral signaling of OEA with effector hypothalamic nuclei. Brain histamine affects feeding behavior in a complex and not fully understood fashion (Fig. 5). It is fundamental for appetitive and aversive responses during motivated behavior (24), and blockade of histamine H_1R in the hypothalamus is believed to be responsible for the weight gain and metabolic dysregulation associated with the clinical use of atypical antipsychotics (25). Several peptides and hormones—such as leptin, corticotropin-, TSH-releasing hormones, and nefastin-1—are satiety modulators acting, at least in part, through histamine neurons activity (26–28). So far, there has been no information regarding brain histamine taking part in the anorexic effects of a modulator that, at the dose used in this study, does not easily pass the blood–brain barrier. Here, by using different experimental settings, we invariably show that chronic or acute histamine deficiency significantly attenuates OEA-induced hypophagia. OEA's effects in normal mice were not completely reversed in HDC-KO or α-FMH–treated mice; indeed, it has been recently proposed that an increase in peripheral fatty acid oxidation and ketogenesis (29), as well as direct activation of the area postrema (30), may contribute to OEA's satiety effects. Nonetheless, our use of different experimental settings gave comparable results, supporting our view that OEA requires the integrity of the histamine system to fully exert its hypophagic effect.

By monitoring the natural progression of feeding behavior and its transition from eating to resting (i.e., satiety occurrence), the BSS can provide a detailed analysis of the structure of feeding behavior (18, 31). With respect to controls and α-FMH–injected animals, OEA administration produced a temporal shifting toward earlier intervals of the cooccurrence of eating and resting behaviors. As illustrated by the preservation of the mutual relationship between feeding and nonfeeding behaviors, OEA induced a robust acceleration of satiety development without disrupting the basic structure of the feeding cycle, whereas histamine depletion abolished OEA-induced premature onset of satiety. Also, the BSS allows the continuous and complete

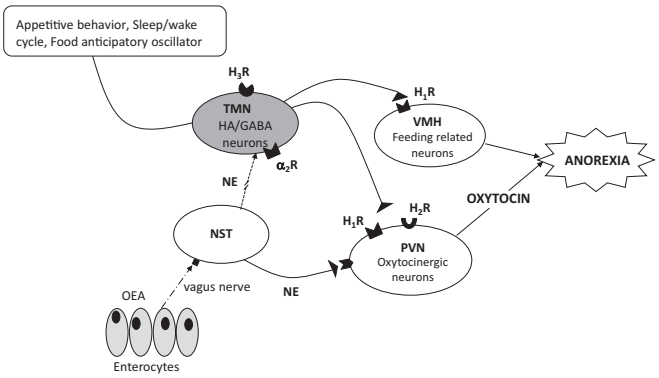

Fig. 5. Schematic drawing illustrating the putative interactions between OEA and the central histaminergic system. Histamine neurons are localized exclusively in the TMN of the posterior hypothalamus. Putative driver and modulatory inputs to the TMN are designated according to (24). The broken line designates presumed noradrenergic excitatory input from the NST to the TMN. According to our hypothesis, OEA induces anorexia indirectly stimulating histamine neurons in the TMN that project to the PVN. Activation of H_1 and H_2 receptors on feeding-related neurons in the PVN stimulates oxytocin release. Histamine mediates suppression of food intake also independently of OEA activating neurons in the VMH (47).

examination of food intake and provides the most accurate and detailed profile of feeding behavior, which are largely superior to interval sampling techniques (18). To understand which brain regions require histamine signaling for OEA-induced hypophagia, we used c-Fos expression as marker of functional activity. We found that lack of central histamine dampens OEA-induced increase of c-Fos expression in oxytocin PVN neurons of HDC-KO mice. The PVN integrates central and peripheral satiety signals, and H_1R activation within the PVN has been implicated in the neuronal regulation of appetite (Fig. 5), as reported by decreased food intake following brain infusion of an H_1R agonist and increased c-Fos–like immunoreactivity within the PVN (10). As pharmacological blockade of oxytocin receptors in the brain prevents OEA anorexic effects (2), we believe that histamine signaling on oxytocic PVN neurons is necessary for OEA to fully exert its anorexic effect (Fig. 5). In this regard, intranuclear and systemic release of oxytocin in response to suckling is controlled by H_1R and H_2R within the PVN (32). It was recently shown that noradrenergic NST–PVN projections are involved in the activation of the hypothalamic oxytocin system (33). In the TMN, α2A adrenoreceptors inhibit GABAergic transmission to TMN neurons (34). It is conceivable that NST adrenergic fibers projecting to the TMN disinhibit TMN neurons that in turn facilitate oxytocin release from the PVN to mediate OEA's prosatiety effect. Indeed, OEA increased c-Fos expression in a subgroup of TMN neurons, corresponding to the E2/E3 region in the mouse (35), that presumably are organized in a functionally distinct circuit, impinging on selected brain regions (36). c-Fos/HDC double-immunoreactive neurons in food-deprived mice were few, which is consistent with results obtained in rats under scheduled feeding (37). Interestingly, we also found that OEA decreased neuronal activity within the nucleus accumbens, as suggested by the low expression of c-Fos in both HDC-KO and WT mice. Although in this context we did not investigate this aspect further, it is interesting that OEA restores gut-stimulated dopamine release in the striatum of high-fat-fed rats increasing the reward value of unpalatable, yet healthier food (38).

As brain histamine signaling in the PVN seems to be involved in the acute effects of OEA on food consumption, we expected OEA to increase brain histamine release. Although technical limitations do not allow performing in vivo microdialysis experiments in the mouse PVN, we found in support of our hypothesis that OEA increased cortical histamine release. We further tested our hypothesis of brain histamine and OEA signaling functional interactions by measuring food consumption after coadministration of OEA and ABT-239, an H_3R antagonist that blocks both auto- and heteroreceptors and increases transiently central release of histamine (12). Previous reports indicate that H_3R antagonists decrease food intake in several mammalian species (reviewed in ref. 39), and here we show for the first time, to our knowledge, such an effect for ABT-239 as well. Furthermore, ABT-239 increased cortical histamine, and in agreement with feeding behavior, we observed a further increase in histamine release following ABT-239 and OEA coadministration. In our model we hypothesize that the hypophagic effects of OEA and ABT-239 converge onto a common pathway, as also strongly suggested by the isobolographic analysis of feeding behavior. Histaminergic neurons may also induce hypophagia by targeting other brain regions not affected by OEA, as is the case of leptin that recruits histamine neurotransmission in the VMH (40). Also, H_3R antagonists and OEA regulate the release of several neurotransmitters other than histamine (41, 42), which may contribute to the hypophagic effects independently of each other.

Recently, Torrealba and coworkers, using a behavioral protocol that separates the appetitive from the consummatory phase of feeding, showed that histamine is differentially involved in these two aspects of feeding behavior and that histamine is important for motivation to eat (20, 21). Brain histamine then seems to have different roles during food anticipatory responses and food consumption (43). Such a complex orchestration may be served by different histamine neuronal subpopulations that are recruited at different times during the unfolding of a specific behavior (36). Histamine neurons send broad projections within the CNS that are organized in functionally distinct circuits impinging on different brain regions (5). This implies independent functions of subsets of histamine neurons according to their terminal projections and their selective participation in different aspects of behavioral responses. It is interesting that OEA elicits histamine release from the cortex of hungry mice, but it is ineffective in satiated animals. To our knowledge, this is the first study to report that endogenous molecules can affect histamine release differentially depending on the homeostatic state of the animal. Whether histamine modulation in the cortex is relevant for satiety to curb the incentive to eat is not known and certainly deserves further study. Our study uncovers the role of brain histamine in the signal transduction of OEA-mediated anorexigenic effects. We believe that understanding the role of the histaminergic system in driving or modulating feeding behavior is of therapeutic relevance; for instance, atypical antipsychotics are thought to cause obesity by targeting histamine H_1R (25), and the orexigenic liability of these drugs parallels their binding potency for histamine H_1R (44, 45). Our results may contribute to the development of more effective pharmacotherapy for the management of obesity and ameliorate the safety profile of centrally acting drugs. In this regard, the first H_3R antagonist for narcolepsy treatment was recently filed with the European Medicine Agency (46), and its effectiveness in obese patients may be assessed.

Materials and Methods

Animals. Male CD1 mice (8–9 wk, 25–35 g; Harlan), HDC-KO mice and WT littermates (129/Sv background; see *SI Materials and Methods* for genotyping procedures and Fig. S5) grown in the animal facility of Dipartimento di Neuroscienze, Psicologia, Area del Farmaco, e Salute del Bambino, were housed in a temperature-controlled room (22 ± 1 °C) with a 12:12-h light–dark cycle (lights on from 0700 to 1900 h), at constant temperature and humidity with a standard diet (4RF21; Mucedola s.r.l.) and freely available water. HDC-KO and WT were used at 2–3 mo of age (25–35 g). Mice were handled for 1 wk before experiments. Housing, animal maintenance, and all experiments were conducted in accordance with the Council Directive of the European Community (86/609/EEC) of the Italian Decreto Legislativo 116 (1992) and National Institutes of Health guidelines on animal care and were approved and supervised by a veterinarian.

Evaluation of Cumulative Food Consumption. Mice were tested during the lights-on (0900 h) or lights-off (1900 h) cycle after 12 h food deprivation while water remained available. A weighed amount of standard chow pellets was placed in the food rack, and food consumption evaluated as the difference in weight between that of initially provided food and that left in the rack, including spillage in the cage. Mice were randomly assigned to the experimental groups. The protocol for cerebral histamine depletion with α-FMH i.c.v. injection is described in detail in *SI Materials and Methods*. Food consumption was measured 15, 30, 45, and 60 min at 2, 4, 6, 8, 10, and 24 h after food presentation. OEA was injected i.p. 15 min before food presentation in 12 h-fasted mice.

Isobolographic Analysis. The interaction between OEA and ABT-239 was evaluated by coadministration of fixed ratios of each drug and by performing an isobolographic analysis as detailed in *SI Materials and Methods*.

BSS Analysis and PWM Intake Assessment. Before α-FMH infusions, mice were habituated for 7 d to a PWM diet. PWM was prepared daily as a mixture of ground standard dry powdered food pellets in sweetened condensed milk (Nestlè) solubilized in distilled water (1:1.5) and offered for 1 h/d (light cycle). To minimize diet spillage, PWM was provided in special feeder beakers. The BSS paradigm was performed as described previously (31) and in *SI Materials and Methods*.

Microdialysis Experiments. The effects of OEA and ABT-239 on brain histamine release were evaluated in freely moving CD1 mice implanted with microdialysis probes. For details on surgery, experimental protocols, and HPLC-fluorimetric assay to quantify histamine, see *SI Materials and Methods*. Experiments are also described in detail in *SI Materials and Methods*.

Immunohistochemistry. HDC-KO and WT littermates were maintained on the standard chow diet and food deprived for 12 h (between 2000 h and 800 h; water remained available) before i.p. administration of OEA (10 mg/kg) or saline. Two hours after injections, mice were deeply anesthetized with chloral hydrate and perfused transcardially with cold physiological saline followed by 4% (vol/vol) paraformaldehyde in 0.1 M phosphate buffer, pH 7.4. Brains were processed for standard immunostaining as detailed in *SI Materials and Methods*.

Data and statistical analysis. Statistical analysis was performed using Prism Software (GraphPad). Statistical significance of cumulative food consumption and histamine release in microdialysis experiments were analyzed by two-way ANOVA (time × treatment) with Bonferroni's post hoc test. Differences in c-Fos expression were determined by one-way ANOVA with Newman–Keuls post hoc test. An unpaired *t* test was used to determine statistical significance between theoretical and experimental ED_{50}, as well as differences between WT and HDC-KO mice in single- and double-labeled PVN and TMN neurons. OEA and α-FMH effects on the duration of each BSS-related behavior were assessed by two-way repeated-measures ANOVAs with treatment (six levels) as the between-subject variable and time (eight levels consisting in eight time bins of 5-min each, from T1 to T8) as the within-subject variable, with Bonferroni's post hoc test. The criterion value for all statistical tests was $P \leq 0.05$.

ACKNOWLEDGMENTS. We thank Roberta Fabbri for technical assistance with confocal microscopy and Liz Muller and Eveline Stolz for assistance with isobolographic analysis. We also thank the National Research Council European Mouse Mutant Archive animal research facility. This work was supported by Programmi di Ricerca di Rilevante Interesse Naziona le Grant 2009 2009ESX7T3_003 E 55.921, Compagnia di San Paolo, and Ente Cassa di Risparmio di Firenze. G.P. was the recipient of the Young Investigator Award.

1. Fu J, et al. (2003) Oleylethanolamide regulates feeding and body weight through activation of the nuclear receptor PPAR-alpha. *Nature* 425(6953):90–93.
2. Gaetani S, et al. (2010) The fat-induced satiety factor OEA suppresses feeding through central release of oxytocin. *J Neusci* 30(24):8096–8101.
3. Romano A, et al. (2013) The satiety signal oleoylethanolamide stimulates oxytocin neurosecretion from rat hypothalamic neurons. *Peptides* 49:21–26.
4. Piomelli D (2013) A fatty gut feeling. *Trends Endocrinol Metab* 24(7):332–341.
5. Giannoni P, et al. (2009) Heterogeneity of histaminergic neurons in the tuberomammillary nucleus of the rat. *Eur J Neurosci* 29(12):2363–2374.
6. Haas H, Panula P (2003) The role of histamine and the tuberomamillary nucleus in the nervous system. *Nat Rev Neurosci* 4(2):121–130.
7. Sakata T, Yoshimatsu H, Kurokawa M (1997) Hypothalamic neuronal histamine: Implications of its homeostatic control of energy metabolism. *Nutrition* 13(5):403–411.
8. Clineschmidt BV, Lotti VJ (1973) Histamine: Intraventricular injection suppresses ingestive behavior of the cat. *Arch Int Pharmacodyn Ther* 206(2):288–298.
9. Lecklin A, Tuomisto L (1998) The blockade of H1 receptors attenuates the suppression of feeding and diuresis induced by inhibition of histamine catabolism. *Pharmacol Biochem Behav* 59(3):753–758.
10. Masaki T, et al. (2004) Involvement of hypothalamic histamine H1 receptor in the regulation of feeding rhythm and obesity. *Diabetes* 53(9):2250–2260.
11. Ookuma K, Yoshimatsu H, Sakata T, Fujimoto K, Fukagawa F (1989) Hypothalamic sites of neuronal histamine action on food intake by rats. *Brain Res* 490(2):268–275.
12. Munari L, Provensi G, Passani MB, Blandina P (2013) Selective brain region activation by histamine H_3 receptor antagonist/inverse agonist ABT-239 enhances acetylcholine and histamine release and increases c-Fos expression. *Neuropharmacology* 70:131–140.
13. Campolongo P, et al. (2009) Fat-induced satiety factor oleoylethanolamide enhances memory consolidation. *Proc Natl Acad Sci USA* 106(19):8027–8031.
14. Proulx K, et al. (2005) Mechanisms of oleoylethanolamide-induced changes in feeding behavior and motor activity. *Am J Physiol Regul Integr Comp Physiol* 289(3):R729–R737.
15. Fülöp AK, et al. (2003) Hyperleptinemia, visceral adiposity, and decreased glucose tolerance in mice with a targeted disruption of the histidine decarboxylase gene. *Endocrinology* 144(10):4306–4314.
16. Takahashi K, Lin JS, Sakai K (2006) Neuronal activity of histaminergic tuberomammillary neurons during wake-sleep states in the mouse. *J Neurosci* 26(40): 10292–10298.
17. Tallarida RJ (2002) The interaction index: A measure of drug synergism. *Pain* 98(1-2): 163–168.
18. Halford JC, Wanninayake SC, Blundell JE (1998) Behavioral satiety sequence (BSS) for the diagnosis of drug action on food intake. *Pharmacol Biochem Behav* 61(2): 159–168.
19. Orofino AG, Ruarte MB, Alvarez EO (1999) Exploratory behaviour after intra-accumbens histamine and/or histamine antagonists injection in the rat. *Behav Brain Res* 102(1-2):171–180.
20. Valdés JL, Maldonado P, Recabarren M, Fuentes R, Torrealba F (2006) The infralimbic cortical area commands the behavioral and vegetative arousal during appetitive behavior in the rat. *Eur J Neurosci* 23(5):1352–1364.
21. Valdés JL, et al. (2010) The histaminergic tuberomammillary nucleus is critical for motivated arousal. *Eur J Neurosci* 31(11):2073–2085.
22. Izzo AA, et al. (2010) Basal and fasting/refeeding-regulated tissue levels of endogenous PPAR-alpha ligands in Zucker rats. *Obesity (Silver Spring)* 18(1):55–62.
23. Gaetani S, Oveisi F, Piomelli D (2003) Modulation of meal pattern in the rat by the anorexic lipid mediator oleoylethanolamide. *Neuropsychopharmacology* 28(7):1311–1316.
24. Torrealba F, Riveros ME, Contreras M, Valdes JL (2012) Histamine and motivation. *Front Syst Neurosci* 6:51.
25. Kim SF, Huang AS, Snowman AM, Teuscher C, Snyder SH (2007) From the cover: Antipsychotic drug-induced weight gain mediated by histamine H1 receptor-linked activation of hypothalamic AMP-kinase. *Proc Natl Acad Sci USA* 104(9):3456–3459.
26. Morimoto T, et al. (1999) Involvement of the histaminergic system in leptin-induced suppression of food intake. *Physiol Behav* 67(5):679–683.
27. Gotoh K, et al. (2005) Glucagon-like peptide-1, corticotropin-releasing hormone, and hypothalamic neuronal histamine interact in the leptin-signaling pathway to regulate feeding behavior. *FASEB J* 19(9):1131–1133.
28. Parmentier R, et al. (2009) Excitation of histaminergic tuberomamillary neurons by thyrotropin-releasing hormone. *J Neurosci* 29(14):4471–4483.
29. Karimian Azari E, et al. (2014) Vagal afferents are not necessary for the satiety effect of the gut lipid messenger oleoylethanolamide (OEA). *Am J Physiol Regul Integr Comp Physiol*, in press.
30. Romano A, et al. (2014) High dietary fat intake influences the activation of specific hindbrain and hypothalamic nuclei by the satiety factor oleoylethanolamide. *Physiol Behav*, 10.1016/j.physbeh.2014.04.039.
31. Coccurello R, et al. (2010) Effects of the increase in neuronal fatty acids availability on food intake and satiety in mice. *Psychopharmacology (Berl)* 210(1):85–95.
32. Bealer SL, Crowley WR (2001) Histaminergic control of oxytocin release in the paraventricular nucleus during lactation in rats. *Exp Neurol* 171(2):317–322.
33. Romano A, et al. (2013) Hindbrain noradrenergic input to the hypothalamic PVN mediates the activation of oxytocinergic neurons induced by the satiety factor oleoylethanolamide. *Am J Physiol Endocrinol Metab* 305(10):E1266–E1273.
34. Nakamura M, Suk K, Lee MG, Jang IS (2013) α(2A) adrenoceptor-mediated presynaptic inhibition of GABAergic transmission in rat tuberomammillary nucleus neurons. *J Neurochem* 125(6):832–842.
35. Rozov SV, Zant JC, Karlstedt K, Porkka-Heiskanen T, Panula P (2014) Periodic properties of the histaminergic system of the mouse brain. *Eur J Neurosci* 39(2):218–228.
36. Blandina P, Munari L, Provensi G, Passani MB (2012) Histamine neurons in the tuberomamillary nucleus: A whole center or distinct subpopulations? *Front Syst Neurosci* 6:33.
37. Umehara H, et al. (2011) Deprivation of anticipated food under scheduled feeding induces c-Fos expression in the caudal part of the arcuate nucleus of hypothalamus through histamine H_1 receptors in rats: Potential involvement of E3 subgroup of histaminergic neurons in tuberomammillary nucleus. *Brain Res* 1387:61–70.
38. Tellez LA, et al. (2013) A gut lipid messenger links excess dietary fat to dopamine deficiency. *Science* 341(6147):800–802.
39. Passani MB, Blandina P (2011) Histamine receptors in the CNS as targets for therapeutic intervention. *Trends Pharmacol Sci* 32(4):242–249.
40. Seth R, Terry DE, Parrish B, Bhatt R, Overton JM (2012) Amylin-leptin coadministration stimulates central histaminergic signaling in rats. *Brain Res* 1442:15–24.
41. Serrano A, et al. (2011) Oleoylethanolamide: Effects on hypothalamic transmitters and gut peptides regulating food intake. *Neuropharmacology* 60(4):593–601.
42. Passani MB, Blandina P, Torrealba F (2011) The histamine H3 receptor and eating behavior. *J Pharmacol Exp Ther* 336(1):24–29.
43. Ishizuka T, Yamatodani A (2012) Integrative role of the histaminergic system in feeding and taste perception. *Front Syst Neurosci* 6:44.
44. Kroeze WK, et al. (2003) H1-histamine receptor affinity predicts short-term weight gain for typical and atypical antipsychotic drugs. *Neuropsychopharmacology* 28(3): 519–526.
45. Coccurello R, Moles A (2010) Potential mechanisms of atypical antipsychotic-induced metabolic derangement: Clues for understanding obesity and novel drug design. *Pharmacol Ther* 127(3):210–251.
46. Dauvilliers Y, et al.; HARMONY I study group (2013) Pitolisant versus placebo or modafinil in patients with narcolepsy: A double-blind, randomised trial. *Lancet Neurol* 12(11):1068–1075.
47. Masaki T, Yoshimatsu H (2006) The hypothalamic H1 receptor: A novel therapeutic target for disrupting diurnal feeding rhythm and obesity. *Trends Pharmacol Sci* 27(5): 279–284.

Supporting Information

Provensi et al. 10.1073/pnas.1322016111

SI Materials and Methods

Chemicals. Oleoylethanolamide (OEA) (Tocris Bioscience) was dissolved in saline/polyethylene glycol/Tween80 (90/5/5, vol/vol/vol). ABT-239 and α-fluoromethylhistidine (α-FMH) were synthesized at Abbott Laboratories and dissolved in physiological saline. All other reagents and solvents were of HPLC grade or the highest grade available (Sigma).

Detection of the Histidine Decarboxylase Gene. In this study we used inbred WT and histidine decarboxylase (HDC)-KO mice descendent from the 129/Sv mouse strain generated by Ohtsu et al. (1). The genotype was determined using the PCR protocol described by Parmentier et al. (2). Briefly, the following primers were used for WT allele amplification: 5′-AGT GAG GGA CTG TGG CTC CAC GTC GAT GCT-3′ (complementary to HDC gene 833–862) and 5′-TAC AGT CAA AGT GTA CCA TCA TCC ACT TGG-3′ (HDC gene 980–951). The expected product size was 147 bp. The mutant allele was amplified using primers located within the Neo^r gene: 5′-AAA CAT CGC ATC GAG CGA GCA CGT ACT CGG-3′ and 5′-ATG TCC TGA TAG CGG TCC GCC ACA CCC AGC-3′, with an expected product size of 244 bp. PCR was performed using 40 cycles of 30 s at 94 °C, 1 min at 64 °C, and 1 min at 72 °C, followed by 1 cycle at 72 °C for 10 min. The whole reaction mix was then fractionated on a 2% agarose gel, and the PCR product was visualized by ethidium bromide staining (Fig. S5).

Surgery and α-Fluoromethylhistidine Interocerebroventricular Infusion. Mice were anesthetized with chloral hydrate (400 mg/kg) and placed on a stereotaxic frame equipped with a mouse adapter and ear bars (Kopf Instruments). Bilateral stainless steel cannulae (7 mm in length, with an OD of 0.5 mm and ID of 0.25 mm) were implanted in the lateral ventricle and fixed to the skull using dental cement. The following coordinates were used according to the mouse brain atlas (3): antero-posterior (AP), −0.3; lateral (L), ±1; dorsoventral (DV), −1. After 7 d recovery, α-FMH was infused into the ventricles with mice placed in their home cage. A stainless steel injection microneedle (2.4 mm length, with an OD of 0.25 mm) was connected through a polyethylene catheter to a 2-μL Hamilton precision syringe and then lowered into the lateral cerebral ventricle (DV 2.4 mm from bregma). α-FMH was delivered via an infusion pump (0.5 μL per side) within 1 min. After infusion, the needle was left in place for an additional 40 s. OEA was administered i.p. 24 h after interocerebroventricular α-FMH infusion; controls received equal volumes of saline.

Isobolographic Analysis. To measure food intake, we presented a preweighed amount of food 15 min after systemic treatments with ABT-239 (1, 3, 6, and 10 mg/kg), OEA (2.5, 5, 10, and 20 mg/kg), or vehicle to overnight-fasted CD1 mice. Food was weighed again after 60 min. Inhibition of food consumption was expressed as a percentage of food intake observed in vehicle-treated mice in the same experimental session (4). ED_{50} values of each compound were obtained from the corresponding log dose–response curve. The interaction between ABT-239 and OEA was evaluated by coadministration of fixed proportions of the ED_{50} obtained for each drug (ratio ABT239/OEA ranging between 0.25/0.25 to 2/2). For the drug mixture, experimental ED_{50} (ED_{50mix}) and its associated confidence intervals were obtained by linear regression analysis of the log dose–response curve and compared with the theoretical additive (ED_{50add}) obtained as

$$ED_{50add} = f \times ED_{50ABT\text{-}239} + (1-f) \times ED_{50OEA}, \quad \textbf{[S1]}$$

and the variance was calculated as

$$VarED_{50add} = f^2 \times VarED_{50ABT\text{-}239} + (1-f)^2 \times VarED_{50OEA}, \quad \textbf{[S2]}$$

where f denotes a fraction of the corresponding ED_{50} in the drug mixture (in our study $f = 0.5$). From these values, confidential intervals were calculated and resolved according to the ratio of the individual drug in the combination (5). When the drug combination gives an experimental ED_{50} not statistically different from the theoretical calculated ED_{50}, the combination is interpreted as having an addictive effect (6). Additionally, to describe the magnitude of interaction, we calculated the interaction index according to the formula

$$\gamma = a/A + b/B, \quad \textbf{[S3]}$$

where A and B are the doses of OEA and ABT-239, respectively, that give the specified effect and a and b are the combination doses that cause the same effect. The quantities in Eq. **S3** were obtained from dose–response curves. The interaction index is a quantitative marker for drug combination that indicates the changed potency of the combination. γ-values ∼1 indicate addictive interaction, values >1 imply an antagonistic interaction, and values <1 indicate a synergistic interaction (7).

Microdialysis Experiments. CD1 mice were placed in a stereotaxic frame under deep anesthesia (5% isoflurane, in oxygen), and a guide cannula (CMA 7; CMA Microdialysis) was inserted in the prefrontal cortex using the following coordinates according to ref. 3: AP, 2.1; L, ±1.0; DV, 1.5. The cannula was fixed to the skull using dental cement. Mice treated with α-FMH were injected in the third ventricle during surgery (coordinates AP, −0.3; L, −1; DV, 2.4). After surgery mice were housed singularly to recover for 24 h. On the experiment day, the dialysis membrane (2 mm, cut off 6 kDa, CMA 7 MD; CMA Microdialysis) replaced the obstructor. The probe was perfused with Ringer's solution (NaCl 147 mM, $CaCl_2$ 2.2 mM, KCl 4.0 mM) for 2 h stabilization (flux = 1 μL/min). After collection of three 30-min baseline samples, OEA (5 mg/kg), ABT-239 (3 mg/kg), or both were injected i.p. Experiments were performed between 900 and 1600 h. To prevent histamine degradation, 1.5 μL 5 mM HCl were added to each sample. Dialysates were immediately frozen and stored at −80 °C until analysis. Cannula placements were verified by post mortem histology. Histamine contents in the dialysates were determined by HPLC-fluorimetry as previously described (8). The sensitivity limit was 10 fmol and the signal-to-noise ratio was higher than 3. Histamine levels in the dialysate samples were calculated in femtomols per 30 minutes.

Histological Verification. Mice were anesthetized with chloral hydrate (400 mg/kg i.p.) and 0.5 μL methylene blue per side was injected in the cannulae. Mice were decapitated and their brains removed and cut in halves along the bregma landmark to verify appropriate dye perfusion through lateral and third ventricles. Three animals were not properly infused and were excluded from the final data analysis. The placement of microdialysis membranes was verified post mortem. Rats were overdosed with chloral hydrate and their brains removed and stored in 10% formalin for 10 d. Forty-micron sections were then sliced on

a cryostat, mounted on gelatin-coated slides, and then stained with cresyl violet for light microscopic observation. Data from rats in which the membranes were not correctly positioned were discarded (less than 10%).

Behavioral Satiety Sequence Analysis and Palatable Wet Mesh Intake Assessment. During palatable wet mesh (PWM) habituation, both body weight and food intake were measured daily. According to the behavioral satiety sequence (BSS) paradigm, eating duration (biting or swallowing food), locomotor activity (movements involving all four limbs and rearing), resting (immobility), and grooming (face and body cleansing and scratching or biting the coat) were continuously recorded for each subject and separately scored. To avoid novel environment stress-induced anxiety, BSS-related behaviors were recorded with animals in their home cages between 1900 and 2000 h, for a total test of 40 min in a soundproof cubicle equipped with an infrared night-vision video recording camera (Panasonic color CCTV Camera WV-CP310/G). Mice were food deprived with water made available for 12 h before each behavioral recording session and randomly assigned to the experimental groups. OEA or vehicle were administered immediately before onset of the dark cycle, and PWM was instantly made available to animals. Each feeder was preweighed and the difference between initial and final weights (after 40 min from the start of BSS test) corresponded to the measure of PWM intake. Onset, duration, and termination of each behavioral event were coded under blind conditions, using EthoVision XT (Version 7) software (Noldus Information Technology Inc.). To analyze behavioral changes in BSS, the 40-min continuous recording for each behavioral category was partitioned into 8 × 5 time bins.

Immunostaining Protocol. Brains were postfixed in the same solution overnight (4 °C), and cryoprotected in 30% sucrose in PB. Forty-micron-thick sections were cut on a cryostat and collected in PB. Sections were preincubated in 0.75% H_2O_2 in PB for 30 min, in 0.2% BSA for 30 min, and then incubated overnight in rabbit c-Fos primary antibodies (1:5,000; Sigma-Aldrich) at 4 °C. The immunoreactive product was detected with an avidin-biotin peroxidase system (Vectastain kit; Vector Laboratories). After washing with PBS, sections were mounted on gelatin-coated slides, dehydrated and coverslipped, and observed using an Olympus BX40 microscope equipped with a Nikon DS-F1 camera. c-Fos immunopositive nuclei were counted bilaterally using the Image J software (National Institutes of Health, Bethesda) on three to six sections per region per mouse and normalized to a 1-mm^2 area according to Munari et al. (8). Atlas coordinates relative to bregma (3) for the sections analyzed were from +1.70 to +1.34 for the infralimbic cortex, from +1.18 to +0.86 for the nucleus accumbens, from −1.46 to −1.70 for the ventromedial hypothalamus, from −0.82 to −0.94 for the paraventricular hypothalamic nucleus (PVN), and from −2.00 to −2.90 for the tuberomammillary nucleus (TMN) that encompass all region subgroups. Statistics were calculated on the average values from three to six sections of individual animals. Thus, sample size and statistics were based on the number of mice. For double-labeling experiments, sections were preincubated with 2% normal goat and donkey sera (NGS and NDS; Jackson Immunoresearch) for 1 h and then incubated in a mixture of c-Fos (1:3,000) and either mouse oxytocin (1:1,000; Millipore) or guinea pig histidine decarboxylase (HDC) (1:400; Acris) primary antibodies with 1% NGS and 1% NDS overnight at 4 °C. Sections were then incubated in Cy3-conjugated donkey anti-rabbit IgG (1:400; Jackson Immunoresearch) for 2 h at room temperature and then in AlexaFluor 488-conjugated, goat anti-mouse IgG, (1:300; Molecular Probes) for 2 h at room temperature. Sections were mounted on glass slides, coverslipped with antifading medium (Vectastain Vector Laboratories), and observed with a Bio-Rad MCR 1024 ES confocal laser scanning microscope (Bio-Rad) equipped with a krypton/argon laser source 15 mW for fluorescence measurements as previously described (9). Single (oxytocin/HDC) and double-labeled (oxytocin/HDC and c-Fos) neurons were counted bilaterally in at least four sections in each PVN/TMN from three mice per experimental group using Image J software. Statistics were calculated on the average values of individual animals. Thus, sample size and statistics were based on the number of mice.

1. Ohtsu H, et al. (2001) Mice lacking histidine decarboxylase exhibit abnormal mast cells. *FEBS Lett* 502(1-2):53–56.
2. Parmentier R, et al. (2002) Anatomical, physiological, and pharmacological characteristics of histidine decarboxylase knock-out mice: Evidence for the role of brain histamine in behavioral and sleep-wake control. *J Neurosci* 22(17):7695–7711.
3. Franklin R, Paxinos G (2007) *The Mouse Brain in Stereotaxic Coordinates* (Academic, New York).
4. Bhavsar S, Watkins J, Young A (1998) Synergy between amylin and cholecystokinin for inhibition of food intake in mice. *Physiol Behav* 64(4):557–561.
5. Stepanović-Petrović RM, et al. (2011) Pharmacological interaction between oxcarbazepine and two COX inhibitors in a rat model of inflammatory hyperalgesia. *Pharmacol Biochem Behav* 97(3):611–618.
6. Tallarida RJ, Stone DJJ, Jr, Raffa RB (1997) Efficient designs for studying synergistic drug combinations. *Life Sci* 61(26):417–425.
7. Tallarida RJ (2002) The interaction index: A measure of drug synergism. *Pain* 98(1-2): 163–168.
8. Munari L, Provensi G, Passani MB, Blandina P (2013) Selective brain region activation by histamine H_3 receptor antagonist/inverse agonist ABT-239 enhances acetylcholine and histamine release and increases c-Fos expression. *Neuropharmacology* 70:131–140.
9. Giannoni P, et al. (2009) Heterogeneity of histaminergic neurons in the tuberomammillary nucleus of the rat. *Eur J Neurosci* 29(12):2363–2374.

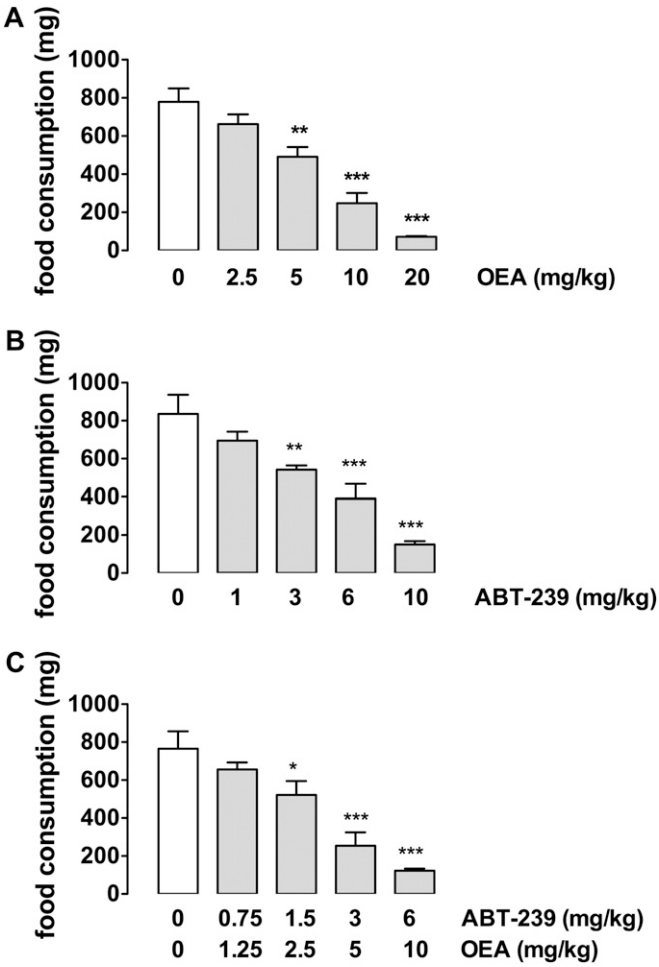

Fig. S1. Hypophagic effects induced by OEA (*A*), ABT-239 (*B*), and OEA–ABT-239 (i.e., combined) (*C*). Twelve hour-fasted CD1 mice received i.p. injection of compounds. Error bars represent mean ± SEM of the quantity of food consumed 1 h after treatments. $n = 5$–9 mice. $^{*}P < 0.05$, $^{**}P < 0.01$, $^{***}P < 0.001$; one-way ANOVA followed by Newman–Keuls.

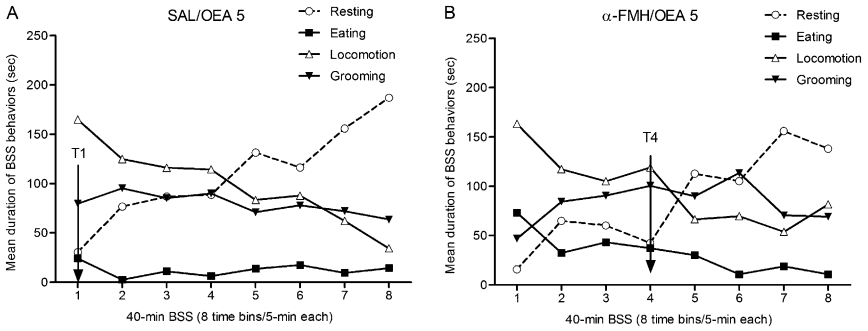

Fig. S2. Temporal development of eating, locomotion, grooming, and resting duration in (*A*) saline/OEA (5 mg/kg) and (*B*) α-FMH/OEA (5 mg/kg). Represented on the *x* axes are eight time bins (T) of 5 min each for a total of 40 min of BSS analysis. Experiments were performed at lights-off (1900 h).

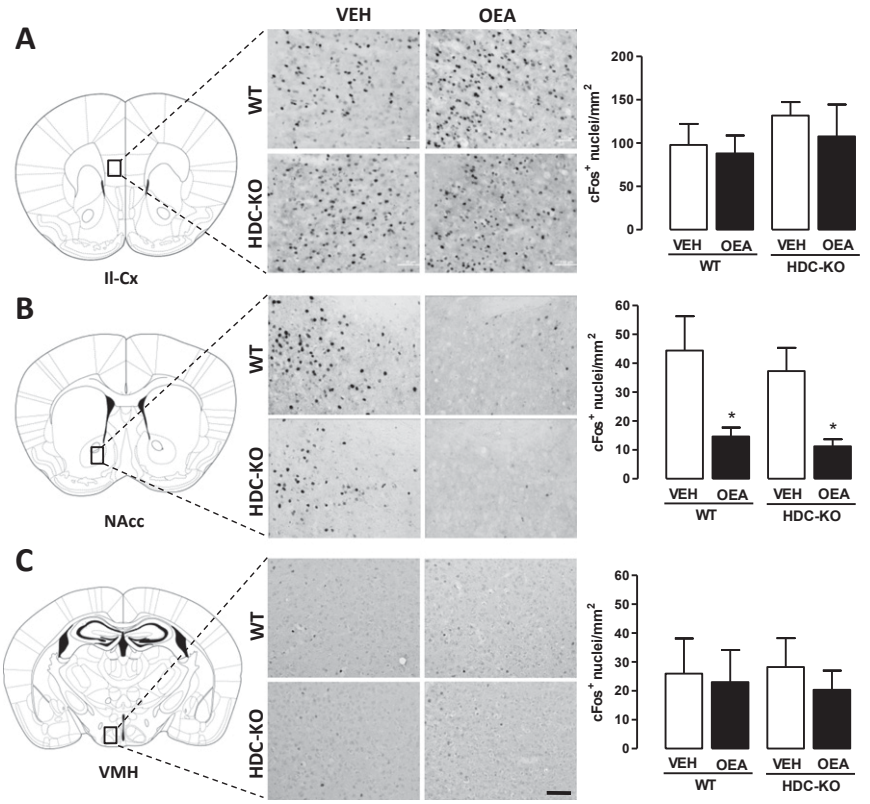

Fig. S3. OEA-induced c-Fos expression in WT and HDC-KO mice. Brain coronal sections showing the effect of vehicle (VEH) or OEA (10 mg/kg) in the infralimbic cortex (*A*), the nucleus accumbens (*B*) and ventromedial hypothalamus (*C*). (Scale bar: 100 μm.) Quantitative data are expressed in the bar graphs as means ±SEM; $*P < 0.05$ vs. respective controls' one-way ANOVA followed by Newman–Keuls. $n = 3$–5 mice per experimental group.

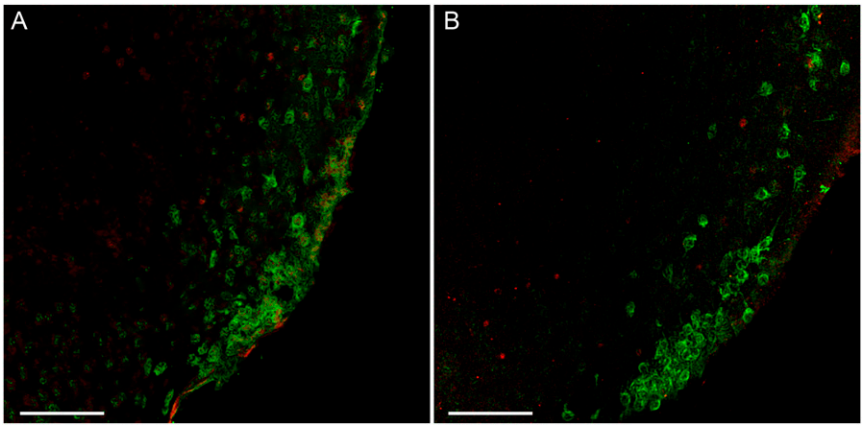

Fig. S4. OEA-induced c-Fos expression in the TMN. Representative brain coronal sections showing the effect of 10 mg/kg OEA (*A*) or vehicle (*B*) on c-Fos protein expression in the TMN of WT mice. This region corresponds the E2/E3 region in the rat (1). $n = 3$ per experimental group. (Scale bars: 100 μm.)

1. Rozov SV, Zant JC, Karlstedt K, Porkka-Heiskanen T, Panula P (2014) Periodic properties of the histaminergic system of the mouse brain. *Eur J Neurosci* 39(2):218–228.

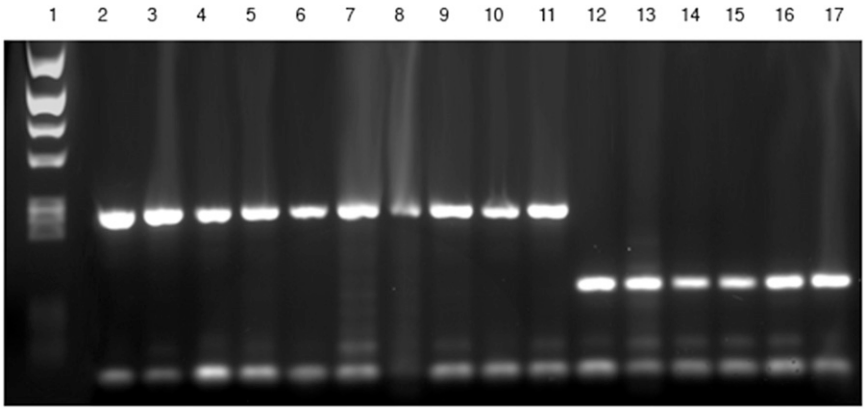

Fig. S5. PCR confirmed the WT and HDC-KO genotypes. Lanes: 1, DNA marker; 2–11, HDC-KO mice; 12–17, WT mice. Note that all WT mice displayed a 147-bp band corresponding to the HDC gene fragment, whereas all HDC-KO mice showed a 244-bp band corresponding to the Neo^r gene fragment.